

# Thermal conductivity measurement of suspended Si-N membranes from 10K to 275K using the 3 omega-Volklein method

Hossein Ftouni, Christophe Blanc, Aurélien Sikora, Jacques Richard, Martial Defoort, Kunal Lulla, Eddy Collin, Olivier Bourgeois

► **To cite this version:**

Hossein Ftouni, Christophe Blanc, Aurélien Sikora, Jacques Richard, Martial Defoort, et al.. Thermal conductivity measurement of suspended Si-N membranes from 10K to 275K using the 3 omega-Volklein method. *Journal of Physics: Conference Series*, IOP Publishing, 2012, 395, pp.012109. <10.1088/1742-6596/395/1/012109>. <hal-00861782>

**HAL Id: hal-00861782**

**<https://hal.archives-ouvertes.fr/hal-00861782>**

Submitted on 3 Nov 2015

**HAL** is a multi-disciplinary open access archive for the deposit and dissemination of scientific research documents, whether they are published or not. The documents may come from teaching and research institutions in France or abroad, or from public or private research centers.

L'archive ouverte pluridisciplinaire **HAL**, est destinée au dépôt et à la diffusion de documents scientifiques de niveau recherche, publiés ou non, émanant des établissements d'enseignement et de recherche français ou étrangers, des laboratoires publics ou privés.

# Thermal conductivity measurement of suspended Si-N membranes from 10 K to 275 K using the $3\omega$ -Völklein method

H Ftouni<sup>1</sup>, C Blanc<sup>1</sup>, A Sikora<sup>1</sup>, J Richard<sup>1</sup>, M Defoort<sup>1</sup>, K Lulla<sup>1</sup>, E Collin<sup>1</sup>, O Bourgeois<sup>1</sup>

<sup>1</sup>Institut NÉEL, CNRS-UJF, 25 avenue des Martyrs, 38042 Grenoble Cedex 9, France

E-mail: [olivier.bourgeois@grenoble.cnrs.fr](mailto:olivier.bourgeois@grenoble.cnrs.fr)

E-mail: [hossein.ftouni@grenoble.cnrs.fr](mailto:hossein.ftouni@grenoble.cnrs.fr)

**Abstract.** The thermal properties of suspended thin films prepared by the micro-machining process have been measured using the  $3\omega$  dynamic method coupled to a Völklein geometry. A transducer (heater/thermometer) centered on the membrane is driven by an ac current causing periodic thermal oscillations. The measurement of the temperature oscillation on the membrane is made at the third harmonic using a Wheatstone bridge set up. Here by coupling the  $3\omega$  method to a Völklein geometry (suspended membrane) we obtained a highly sensitive technique to measure the thermal conductance with a resolution of ( $\Delta K/K = 10^{-3}$ ) and a sensitivity of the order of nanoWatt/K, thanks to a very sensitive niobium nitride thermometry. This method is applied to measure the in-plane thermal conductivity of 100 nm silicon nitride membrane, in the temperature range of 10-275 K.

## 1. Introduction

Membrane heat conduction has always been a key issue in the study of the thermal transfer in low dimensional structures [1]. The reduction in the contribution of phonon to the thermal conductivity is a very active subject of research [2, 3, 4]. Reduced size effects are studied on the heat conduction or heat storage (heat capacity) [5, 6], but also on the phonon mean free path [7], on the dispersion relation [8] or on the transmission coefficient [2, 9]. This confinement effect may have significant consequences in the thermal properties of phononic crystals, nanoparticles embedded in a matrix, nanomembranes or in the presence of rough surfaces etc... Therefore there is growing need for thermal characterization of grown thin films where the thermal properties may strongly depend along which axis they are measured. Hence, their measurements need adapted experimental techniques from high temperature [1] to low temperature [10].

The need for precise measurements of very thin films or membranes imposes to work with suspended systems. However, very few techniques permit such achievement on membrane and nanowire [11, 12, 13, 14], especially when a high sensitivity is necessary. Here we report on a very sensitive dynamic method based on a mix of the Völklein and the  $3\omega$  methods to measure the in-plane thermal conductance of membranes [15, 16]. The sensor is constituted by a thin rectangular suspended membrane with a highly sensitive thermometer lithographed in the center of the membrane. The thermal gradient is established between the center of the membrane and

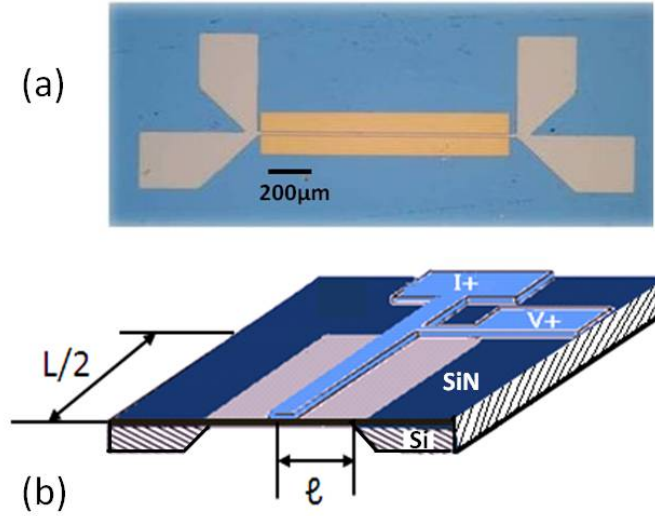


**Figure 1.** Pattern of the heater/thermometer line on the SiN membrane (a). Cross section schematic of the Völklein geometry (b). The width of the heater/thermometre line is typically  $20\mu\text{m}$ , the width of the membrane is equal to  $200\mu\text{m}$  and the length (1.0mm).

the frame which is regulated in temperature. The thermal conductance is deduced from the voltage signal measured at the third harmonic appearing across the transducer.

## 2. Experimental

The measurement system is constituted by a heater-thermometer centered along the long axis of a rectangular membrane as shown in Fig.1. The principle of the method is as follows: a sinusoidal Joule heating is generated by an a.c. electric current flowing across a transducer and then a temperature oscillation appears. The center of the membrane is thermally isolated from the frame and hence its temperature is free to increase. The amplitude of the temperature increase or its dependence on the frequency of the excitation is entirely related to the thermal properties of the membrane. By measuring the  $V_{3\omega}$  voltage appearing across the transducer, it is possible to deduce the thermal conductivity and the specific heat. The transducer is made out of a material (NbN niobium nitride) whose resistance is strongly temperature dependant, see Fig.2.a. It serves as a thermometer and heater at the same time.

The amorphous SiN film, which have the advantage to be KOH resistant, are grown on both side of a silicon substrate by chemical vapor deposition. The 1 mm long and  $200\mu\text{m}$  large membranes are patterned on the rear side by photolithography. After removing the silicon nitride by  $\text{SF}_6$  Reactive Ion Etching, the exposed silicon on the rear side is removed in KOH etching. Finally, rectangular SiN membranes are obtained on the front side.

The transducers are patterned on the membranes using regular clean room processes. They consist of niobium nitride and are grown using a dc-pulsed magnetron sputtering from a high purity (99%) Nb target in a mixture of Ar/ $\text{N}_2$ [17]. Depending on the stoichiometry, the electrical properties of the NbN can vary a lot. The thermometer has been designed to be sensitive in the 10 K-300 K temperature range. The resistance of the thermometer is calibrated using a standard four probe technique between 4 K and 300 K in a  $^4\text{He}$  cryostat.

The voltage drop across the thermometer line has a small component at  $3\omega$  which is much smaller than the  $1\omega$  signal by a factor of  $10^4/10^5$ . In the following, we explain how by using a specific Wheatstone bridge [18] we strongly reduce the component of the measured

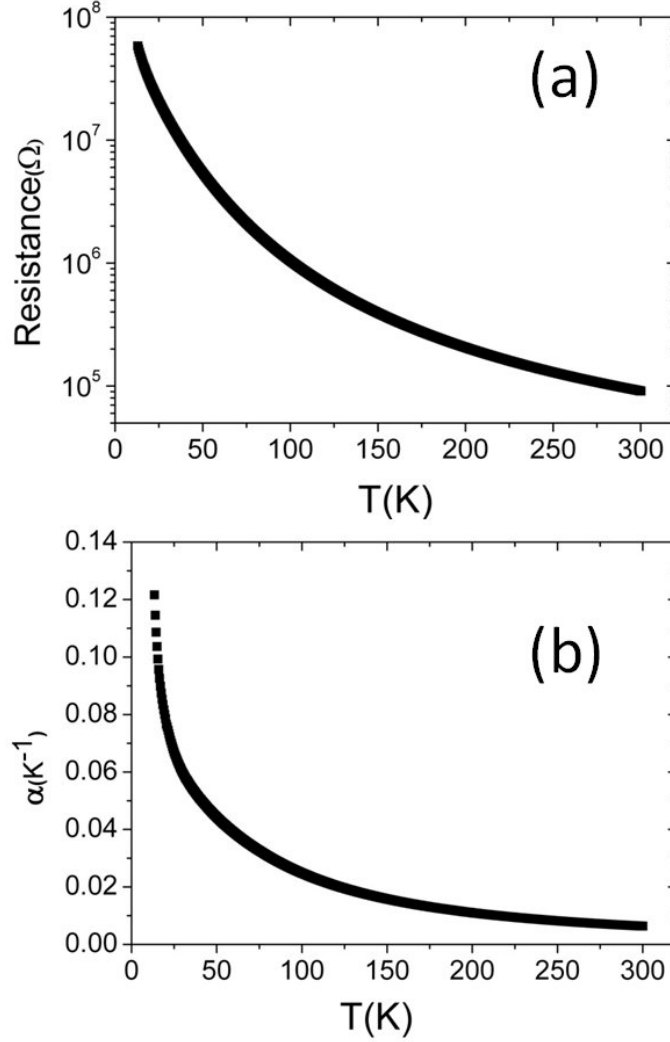


**Figure 2.** Evolution of the resistance (a) and the temperature coefficient of resistance (b) of the thermometer  $R_e$  as a function of the temperature.

voltage at angular frequency  $1\omega$ . The bridge consists of the measured sample (resistance  $R_e$ ), which is the NbN thermometer on the SiN membrane, the reference thermometer ( $R_{ref}$ ), an adjustable resistor  $R_v$  and an equivalent non adjustable resistor  $R_1 = 50k\Omega$  as schematized on the Fig.3. The NbN reference thermometer (or reference transducer) has the same geometry and is deposited in the same run as the transducer on the membrane.

The temperature coefficient  $\alpha = -\frac{1}{R} \frac{dR}{dT}$ , shown on the bottom panel of the Fig.2.b reaches  $10^{-1}$  at low temperature and  $10^{-2}$  at room temperature, a very high value as compared to regular thermometer like platinum. The two resistors  $R_v$  and  $R_1$  are positioned outside the cryogenic system. If  $R_e = R_{ref}$  and  $R_1 = R_v$ , the electrical potential at angular frequency  $\omega$  is the same in C and D. Consequently, there is no voltage at the angular frequency  $\omega$  between C and D. Since the reference thermometer is not on the membrane, its temperature remains at the regulated temperature of the bath  $T_b$  therefore its resistance does not change. The elevation of temperature of the reference transducer has been estimated to be much less than  $10^{-6}K$  [19]. Therefore the bulk silicon underneath the SIN thin film can be considered as an infinite

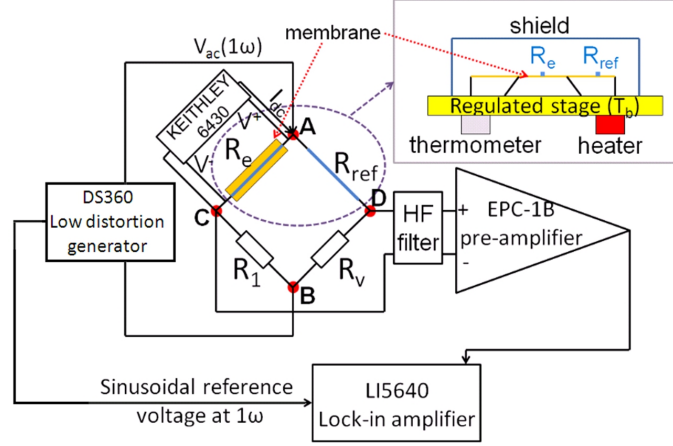


**Figure 3.** Schematic of the electrical measurement system including HF filter, preamplifier and lock-in amplifier. A, B, C and D represent the nodes of the Wheatstone bridge. The  $V_{3\omega}$  is measured between C and D. The transducer is referred as  $R_e$  and the reference resistance as  $R_{ref}$ . The insert presents a schematic of the membrane fixed on the temperature regulated stage covered by the thermal copper shield.

reservoir as compared to the suspended membrane. Thus, it is possible to measure the  $V_{3\omega}$  signal between C and D without the  $1\omega$  component saturating the dynamic reserve of the lock-in amplifier. The two NbN thermometers have practically the same temperature behavior as they have been deposited simultaneously on the SiN substrate. However, due to the presence of inhomogeneity in the deposition process, there is a slight difference of resistance. Thus the  $R_v$  resistor is used to balance the bridge. Thanks to the Wheatstone bridge, the  $V_{3\omega}$  signal is larger than to the  $V_{1\omega}$  signal. The parasitic  $V_{1\omega}$  component has been reduced by a factor of  $10^5$ .

The heating current is generated by applying an alternative voltage of the order of 1 Volt  $V_{ac}$  between A and B with the oscillation output of the DS 360 low distortion generator from Stanford Research Systems. The measured voltage is frequency filtered (for  $f \geq 50$  kHz) and preamplified by a factor of 100 with a low noise preamplifier EPC-1B [20]. EPC-1B is a preamplifier developed at the Institut Néel with an input noise around  $1 \text{ nV}/\sqrt{\text{Hz}}$  between 1 Hz and 1 kHz.

The membrane is installed on a temperature regulated stage and protected by a thermal shield as schematized on the insert of the Fig.3. The copper shield, which is maintained at a temperature close to  $T_b$ , reduces strongly the radiation heat transfer. The thermal gradient between the thermal shield and the sample has been estimated to be much less than 1K, giving a power of 1Watt per meter square exchanged between the membrane and the shield. This is equivalent to a parasitic thermal conductance of  $10^{-7} \text{ Wm}^{-1} \text{ K}^{-1}$ . Consequently, any radiative heat transfer will be neglected in the following. The stage temperature is regulated with a stability of the order of few milliKelvin. The stage temperature  $T_b$  can be regulated from 10 K to room temperature.

### 3. Thermal model of the system

A cross section of the membrane is represented in the Fig.4a. As there is a symmetric axis (the middle of the transducer) the thermal system can be modeled using half the membrane and half the heating power. For simplification, as the membrane is thin ( $e \leq 100$  nm), we assume that the part of the membrane just below the NbN transducer is heated like the thermometer. As the membrane is suspended in vacuum, we assume that the heat can only diffuse along the membrane

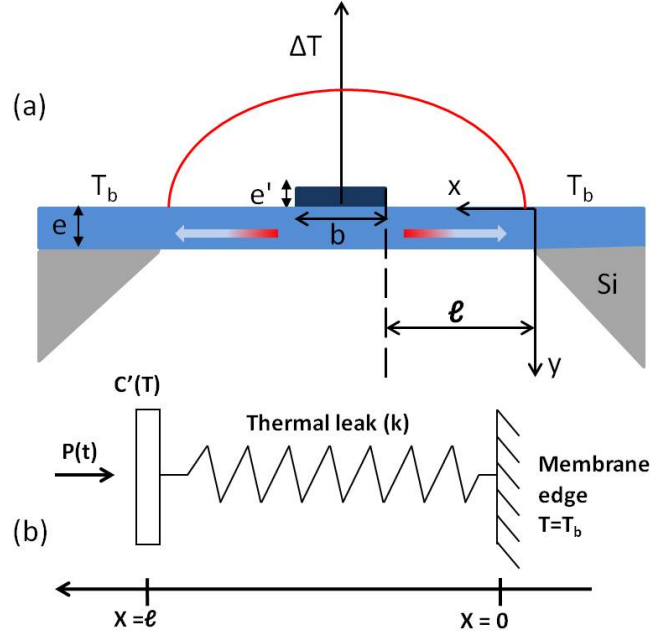


**Figure 4.** (a) Schematic of the membrane on which the NbN transducer is deposited.  $e$  is the thickness of the membrane and  $e'$  the thickness of the NbN transducer. (b) Schematic of the thermal system.

toward the silicon substrate which is at constant temperature  $T_b$ . Thus, in first approximation, we consider a one-dimensional model where the radiative heat loss is neglected thanks to the thermal shield (between the sample and the measurement cell walls), see Fig.3. Therefore, the system is modeled as a volume of matter with a total specific heat  $C'$  and bonded to the thermal bath by the membrane with a thermal conductivity  $k$ . The thermal system is schematized in the Fig.4b. The total specific heat  $C'$  take into account both the NbN thermometer and the part of the membrane below the transducer:

$$C' = \rho_{NbN} c_{NbN} L e' \frac{b}{2} + c \rho \frac{b}{2} L e \quad (1)$$

with  $c$  the specific heat and  $\rho$  the density of the silicon nitride and  $L$  the length of the thermometer line. The temperature is given by the 1D heat diffusion equation:

$$\frac{\partial^2 T(x, t)}{\partial x^2} = \frac{1}{D} \frac{\partial T(x, t)}{\partial t} \quad (2)$$

with  $D$  the diffusivity of the SiN. Calculations using a 2D model give approximately the same results.

In order to calculate the solution of Eq. 2, we need initial and boundary conditions. Therefore, we assume that at  $t=0$ , the temperature of the membrane is  $T_b$  since the transducer is not heated. Moreover, we assume that the membrane edge is always at  $T=T_b$ . Thus, the boundary condition can be written as:  $T(x=0, t) = T_b$ . Moreover, the total dissipated power  $P(t)$  is used to heat both the thermometer and the part of the membrane under the thermometer, and the rest of the membrane:  $C'(T) \frac{\partial T(x, t)}{\partial t} \Big|_{x=\ell} = P(t) - e L \kappa \frac{\partial T}{\partial x} \Big|_{x=\ell}$ .

The general solution of Eq. 2, is:

$$T(x, t) = \frac{P_0 sh[\omega'(1+j)x] e^{j2\omega t}}{(1+j)Sk\omega'ch[\omega'(1+j)\ell] + j2C'\omega sh[w'(1+j)\ell]} \quad (3)$$

with  $\omega' = \sqrt{\frac{\omega}{D}}$ ,  $S=eL$ ,  $P_0=\frac{RI_0^2}{4}$  and  $I = I_0 \sin(\omega t)$ . After development in Taylor expansion in first order in  $\omega$ , the expression of the absolute value of the temperature  $T_m(\ell)$  can be written as followed:

$$T_m(\ell) = \frac{P_0}{K_p \left[ 1 + \omega^2 \left( 4\tau^2 + \frac{2\ell^4}{3D^2} + \frac{4\tau\ell^2}{3D} \right) \right]^{1/2}} \quad (4)$$

with  $K_p=\frac{kS}{\ell}$ ,  $\tau=\frac{C'}{K_p}$ ,  $D$  the thermal diffusivity and  $P_0$  the power dissipated by Joule effect through the membrane (see Fig.4).

The thermal voltage generated across the thermometer is given by:

$$U_{3\omega}(\omega) = R_e \alpha T(\ell, t) I \quad (5)$$

with  $I$  the current coming through the  $R_e$  resistance. Then, the general expression of  $V_{3\omega}$ , between C and D, can be written as follows:

$$|V_{3\omega}^{rms}(\omega)| = \frac{\alpha(V_{ac}^{rms})^3 (R_1 + R_v) R_e^2}{2K_p (R_1 + R_e)^3 (R_1 + R_v + R_{ref}) \left[ 1 + \omega^2 \left( 4\tau^2 + \frac{2\ell^4}{3D^2} + \frac{4\tau\ell^2}{3D} \right) \right]^{1/2}} \quad (6)$$

Where  $V_{ac}^{rms}$  is the voltage applied across the Wheatstone bridge (between A and B) and  $R_1$ ,  $R_v$  the bridge resistances (see Fig.3). At low frequency, the  $\omega$  term becomes negligible and the expression of  $V_{3\omega}$  can be written in its simpler form as:

$$|V_{3\omega}^{rms}(\omega)| = \frac{\alpha(V_{ac}^{rms})^3 (R_1 + R_v) R_e^2}{2K_p (R_1 + R_e)^3 (R_1 + R_v + R_{ref})} \quad (7)$$

Thus, at low frequency,  $V_{3\omega}(f)$  is constant as a function of the frequency and depends on the thermal conductivity  $k$  of the membrane. After the calibration of  $R_e$  and  $R_{ref}$ ,  $R_1$  and  $R_v$  being fixed, a measure of  $V_{3\omega}$  at low frequency allows the calculation of the thermal conductance  $K_p$  using Eq. 7 and hence the thermal conductivity  $k$ .

#### 4. Results

The method has been checked using two different measurements. According to equation 7, the  $V_{3\omega}$  signal depends on the cube of the Wheatstone bridge voltage  $V_{ac}$ . Thus, the  $V_{3\omega}$  signal has been measured at different temperatures to check this behaviour. As an example, the 200 K measurement can be seen on the Fig.5. The linear fit gives a slope very close to 3 which confirms the cubic behaviour of the  $V_{3\omega}$  signal versus the applied voltage  $V_{ac}$ .

The second way of verification requires a frequency scan measurement. According to the equation 6, the  $V_{3\omega}$  signal depends strongly on the angular frequency  $\omega$ . At low frequency the square root term tends to 1 and consequently, the  $V_{3\omega}$  signal becomes constant. As predicted by the theory, a plateau is observed at low frequency for the  $V_{3\omega}$  signal (not shown). The thermal conductivity  $k$  can be extracted from the low frequency plateau thanks to the equation 7.

The thermal conductivity of the silicon nitride membrane has been measured between 10 and 275 K. The results for a 100 nm thick silicon nitride membrane are shown in the Fig.6.

The general behaviour is an increase of the thermal conductivity as the temperature is increased, a usual trend reported in the literature for amorphous silicon nitride films [12, 21, 22].

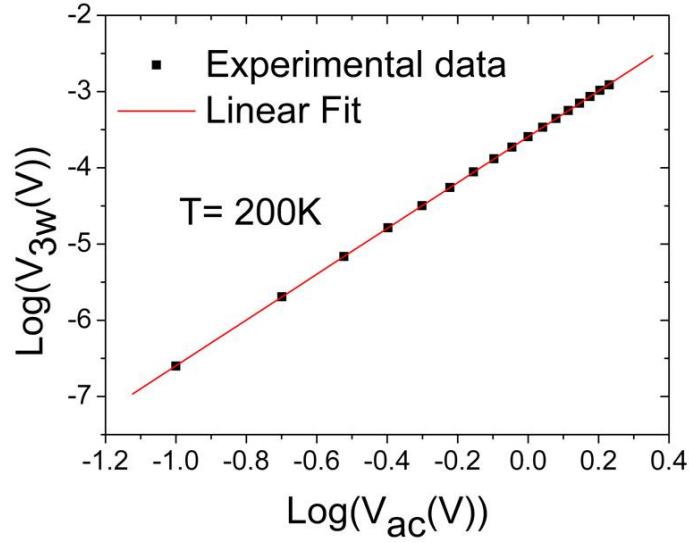


**Figure 5.**  $V_{3\omega}$  signal as a function of the voltage applied across the Wheatstone bridge ( $V_{ac}$ ) in logarithmic scales.

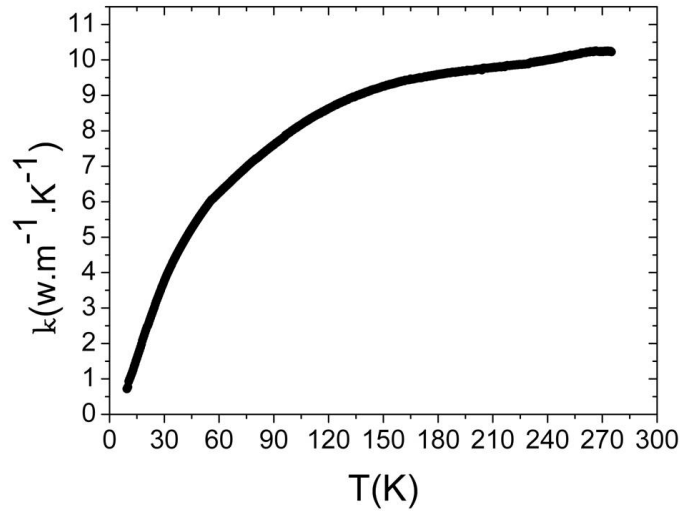


**Figure 6.** Thermal conductivity of a 100 nm thick SiN membrane as a function of the temperature from 10 to 275K.

A value close to  $10 \text{ Wm}^{-1}\text{K}^{-1}$  is obtained at room temperature in agreement with previous measurements of thermal conductivity on thin silicon nitride membranes [12, 23]. The experimental values of the thermal conductance  $K_p$  are measured with high sensitivity  $\Delta K$  that corresponding to  $10^{-9} \text{ W/K}$  and  $10^{-8} \text{ W/K}$  at 10 K and 275 K respectively, along with a resolution of  $\Delta K/K = 10^{-3}$ . The power sensitivity at room temperature is below the nanoWatt.

## 5. Conclusion

We have demonstrated a method to measure thermal conductivity of very thin suspended membranes based on a mix of the  $3\omega$  method and the Völklein method. The performances

of the thermometry as well as the measurement chain have been optimized to obtain a very sensitive technique (down to few tenths of nanoWatt) with a resolution of approximately  $10^{-3}$ . As an illustration of the technique, 100 nm thick silicon nitride membranes as well have been measured. By adapting the thermometry, measurement from 0.4 K to 400 K can be done easily.

This method can now be used to measure the in-plane thermal conductivity of various dielectric suspended materials or membranes. This technique will be adapted to very low temperatures to study dielectric suspended structures. Especially, this opens up very exciting possibilities for the study of thermal and mechanical properties of amorphous materials below 10 K. Coupling nanomechanics and nanothermal measurements [24, 25] will bring new insights into the still very open subject of phonon transport in silicon nitride materials.

### Acknowledgments

We acknowledge technical support from Nanofab, Cryogenic shop, Electronic shop and Capthermal for these experiments. Funding for this project was provided by a grant from La Région Rhône-Alpes (Cible and CMIRA) and by the Agence Nationale de la Recherche (ANR) through the project QNM. We would like to thank P. Gandit, P. Brosse-Marion, B. Fernandez, T. Fournier, E. André, P. Lachkar, J.-L. Garden for help and fruitful scientific exchanges.

### References

- [1] D. G. Cahill, W. K. Ford, K. E. Goodson, G. D. Mahan, A. Majumdar, H. J. Maris, R. Merlin, and S. R. Phillpot, *J. Appl. Phys.* **93**, 793 (2003).
- [2] Y. Duchemin and D. Donadio, *Phys. Rev. B* **84**, 115423 (2011).
- [3] J. S. Heron, C. Bera, T. Fournier, N. Mingo and O. Bourgeois, *Phys. Rev. B* **82**, 155458 (2010).
- [4] G. Pernot *et al.*, *Nature Materials* **9**, 491 (2010).
- [5] F.R. Ong, O. Bourgeois, S. Skipetrov, and J. Chaussy, *Phys. Rev. B* **74**, 140503(R) (2006)
- [6] F.R. Ong and O. Bourgeois, *Europhys. Lett.* **79**, 67003 (2007).
- [7] A.J. Minnich, J.A. Johnson, A.J. Schmidt, K. Esfarjani, M.S. Dresselhaus, K.A. Nelson and G.Chen, *Phys. Rev. Lett.* **107**, 095901 (2011).
- [8] N. Mingo, *Phys. Rev. B* **68**, 133308 (2003).
- [9] Y. Chalopin, J.-N. Gillet, S. Volz, *Phys. Rev. B* **77**, 233309 (2008)
- [10] O. Bourgeois, *Topics in Applied Physics* **118**, 537 (2009).
- [11] F. Völklein, *Thin solid Films* **188**, 27 (1990).
- [12] A. Jain and K. E. Goodson, *Journal of Heat Transfer* **130**, 102402 (2008).
- [13] L. Lu, W. Yi and D.L. Zhang, *Rev. Sci. Instrum.* **72**, 2996 (2001).
- [14] O. Bourgeois, T. Fournier and J. Chaussy, *J. Appl. Phys.* **101**, 016104 (2007)
- [15] M. Molina Ruiz, A.F. Lopeandia, F. Pi, D. Givord, O. Bourgeois, and J. Rodriguez-Viejo, *Physical Review B* **83**, 140407(R) (2011).
- [16] J.-L. Garden, H. Guillou, A.F. Lopeandia, J. Richard, J.-S. Heron, G.M. Souche, F.R. Ong, O. Bourgeois, *Thermochimica Acta* **492**, 16 (2009).
- [17] O. Bourgeois, E. André, C. Macovei and J. Chaussy, *Rev. Sci. Instrum.* **77**, 126108 (2006).
- [18] N. O. Birge and S. R. Nagel, *Rev. Sci. Instrum.* **58**, 1464 (1987).
- [19] D.G. Cahill, M. Katiyar, J.R. Abelson, *Phys. Rev. B* **50**, 6077 (1994).
- [20] EPC1B preamplifier has been developed at the Institut Néel and commercialized by Celians-C3EM.
- [21] R. Sultan, A.D. Avery, G. Stiehl, and B.L. Zink, *J. Appl. Phys.* **105**, 043501 (2009).
- [22] D.R. Queen and F. Hellman, *Rev. Sci. Instrum.* **80**, 063901 (2009).
- [23] B. L. Zink, B. Revaz, J. J. Cherry, and F. Hellman, *Rev. Sci. Instrum.* **76**, 024901 (2005).
- [24] M. Defoort, K. Lulla, J.-S. Heron, O. Bourgeois, E. Collin, and F. Pistolesi, *Appl. Phys. Lett.* **99**, 233107 (2011).
- [25] E. Collin, T. Moutonet, J.-S. Heron, O. Bourgeois, Yu. M. Bunkov, and H. Godfrin, *Physical Review B* **84**, 054108 (2011).